

Laser interferometric dilatometer at low temperatures: application to fused silica SRM 739

M. Okaji, N. Yamada, K. Nara and H. Kato

National Research Laboratory of Metrology, 1-1-4, Umezono, Tsukuba 305, Japan

Received 23 March 1995

An optical heterodyne interferometer has been combined with a helium flow cryostat to measure the linear thermal expansion coefficient of solids at cryogenic temperatures. The absolute accuracy in length measurement is within a few nanometres. Measurement results on a specimen of fused silica (SRM 739; by US NIST) in the temperature range 6–273 K are presented and compared with some literature data.

Keywords: thermal expansion; interferometer; instrumentation; fused silica; standard reference material

Accurate determination of the linear thermal expansion coefficient (LTEC) over a wide temperature range is one of the most important requirements not only in the field of materials science but also in the field of industrial technology. The LTEC is especially important in cryogenic engineering, because most cryogenic instruments are made from combinations of materials with different levels of expansion, so that fairly large internal thermal stresses should be generated in such instruments with temperature changes. However, there are not many reliable publications for precise low temperature data. Our aim is to develop an instrument which is capable of making an absolute measurement of the thermal expansivity of cryogenic materials, including reference materials.

In dilatometry, length measurement is made using several methods, such as a push-rod, thermomechanical analysis, a mechanical lever, an optical lever, capacitance, X-rays and optical interferometry. Most of the mechanical methods are convenient, but are generally relative and do not have very high accuracy. X-ray dilatometry is based on an absolute determination of lattice parameters, but normally has poor sensitivity. The capacitance method is highly sensitive especially at cryogenic temperatures, but is a relative method and its accuracy tends to decrease with increase in temperature. Ordinary optical interferometry is essentially an absolute method but is not recognized as a highly sensitive one. However, its sensitivity has been considerably improved with the application of a polarization method¹ and an optical heterodyne method^{2,3} to achieve nanometre range resolution in length measurement.

We have constructed an absolute cryogenic dilatometer utilizing an optical heterodyne interferometer with a helium continuous flow cryostat. The basic design of the interferometric system is similar to that presented in our previous

publications on intermediate and high temperature dilatometry^{3–6}. In the present work, the interferometer was partly modified to realize a more compact optical configuration with better linearity in the fringe detection. The continuous flow cryostat is adopted here to give rapid temperature cooling/heating of the specimen system, very low cryogen consumption and easy optical alignment of the interferometer. We evaluated the performance of the present dilatometer by measuring fused silica specimens supplied by NIST (code number SRM 739; with NIST Certificate between 80 and 1000 K⁷). The measured data were compared with previously reported data, including NIST's certified data.

Dilatometer design

Length measurement system

The light source used in the experiment is a so-called stabilized transverse Zeeman He–Ne laser (Asahi Bunko Co., STZL-1). Its frequency stability is a few parts in 10^{-9} over a few days, which is sufficient to obtain 1 nm resolution for a 10–20 mm difference between two optical path lengths. An absolute wavelength of the laser was calibrated to be $0.6329914 \mu\text{m}$ in vacuum by using a standard iodine stabilized laser at NRLM. The output power from the laser is ≈ 2 mW.

The optical interferometer is basically similar to that developed for middle and high temperature dilatometers^{3–6}. For the convenience of the reader, we present here a brief explanation on the interferometer system. A schematic diagram of the interferometer is shown in *Figure 1*. It consists of two polarized beam splitters (PBS-1 and PBS-2), a half-wave plate (HWP), a quarter-wave plate (QWP), a corner cube prism (CCP), a front reflector (FR) and a back

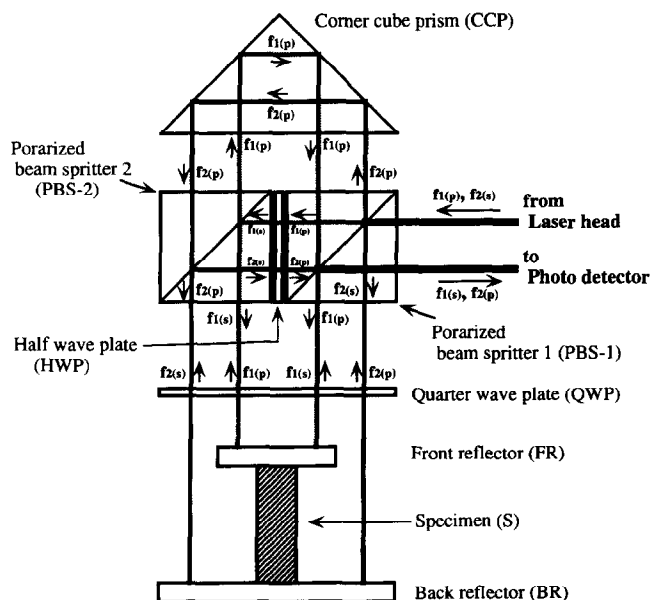


Figure 1 Schematic diagram of double path interferometer

reflector (BR). An incident beam from the Zeeman laser has two slightly different frequency components, f_1 and f_2 , which are characterized by linearly polarizing planes orthogonal to each other (specified by the letters s and p, vertical and horizontal to the drawing plane, respectively). The frequency difference between the two components is ≈ 100 kHz, which is used as the beat frequency for the heterodyne interferometry.

The actual optical paths in the present system are given in Figures 2a, b and c. The optical configuration was modified from the old version as in Figure 1 (single plane configuration of the light beams) to a new one as in Figure 2 (square configuration of the beams), to obtain a more compact arrangement suitable for the small cryogenic specimen cell. The two components are divided and made parallel by the polarized beam splitters (PBS-1, PBS-2), separated by the half-wave plate (HWP). Each beam is reflected by the front reflector (FR) and the back reflector (BR), respectively (Figure 2a). The quarter-wave plate (QWP) is oriented so that the polarized plane of each beam is rotated 90° before and after one reflection. Accordingly, the two parallel beams are transmitted and reflected between the original beam splitters (PBS-1, PBS-2) and the front and back reflectors without losing intensity of light. These two beams are folded by exactly 180° by the corner cube prism (CCP), then trace the second transmission/reflection paths (Figure 2b) and are finally recombined by the same polarized beam splitters (PBS-1, PBS-2) (Figure 2c). The interferometer involves a self-compensation mechanism for optical misalignment such as tilt of the specimen system owing to a combination of the CCP and the double-path configuration. It also involves easy optical alignment and a wide tolerance of non-parallelism between the two reflectors.

In optical heterodyne interferometry, the interference intensity between two electric fields, $A_1 \sin(2\pi f_1 t + \phi_1)$ and $A_2 \sin(2\pi f_2 t + \phi_2)$, is expressed by the following equation

$$I = (A_1^2 + A_2^2)/2 + 2A_1 A_2 \cos(2\pi \Delta f t + \Delta \phi) \quad (1)$$

where $\Delta f = f_1 - f_2$, and $\Delta \phi = \phi_1 - \phi_2$. Accordingly, a phase change of the interferometer can be obtained with high sen-

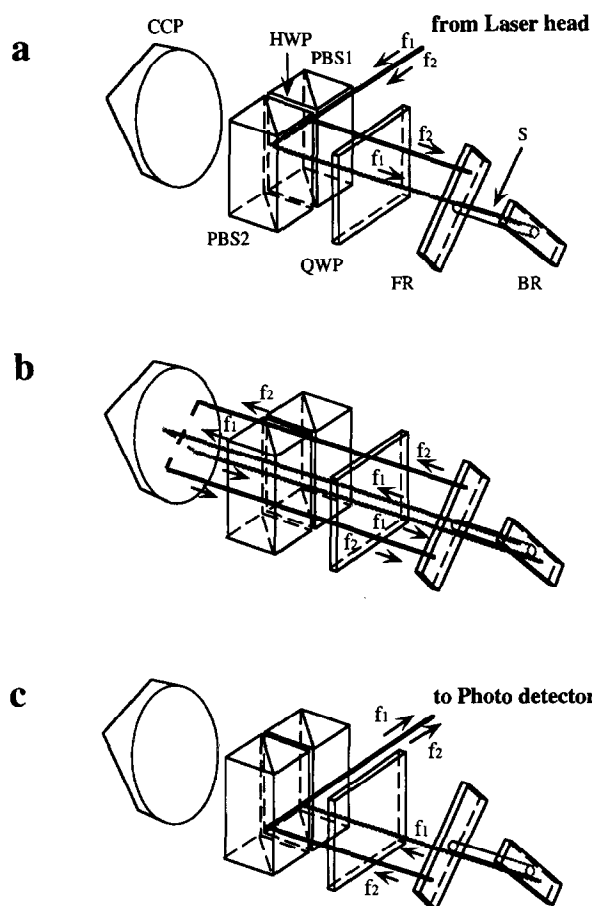


Figure 2 Optical paths of the interferometer, represented in three steps, a, b and c

sitivity by lock-in detection. In the present experiment, the interference beat signal from the interferometer and the reference signal directly from the laser head are both fed to a digital lock-in amplifier (EG & G Inc., Model 5210). The specimen length change can therefore be detected as a relative phase change between these signals. The r.m.s. noise level of phase measurement is 0.5° , which corresponds to a resolution of 0.25 nm in the specimen length change.

In our previous interferometer, some amount of cyclic error (which sometimes reached up to $\pm 10^\circ$ in phase detection) has been observed. This was due to a mixing effect between two frequencies for the heterodyne interferometry. Such mixing was caused by imperfections in the extinction of the polarization characteristics of the polarized beam splitters and misorientation of the optical axis between the incident beam from the laser and the PBS. However, this effect is minimized to the order of $\pm 2^\circ$ by choosing certain PBSs having a very high polarized extinction ratio and optimizing the optical axis of the system. This corresponds to the order of ± 1 nm in length measurement ($\pm 0.01 \times 10^{-6} \text{ K}^{-1}$ LTEC for a 10–20 mm long specimen with a 10 K temperature interval), which is sufficient for the present experiment.

Cryostat system

In designing the cryostat system, the main requirements were easy optical alignment for the interferometer system, arbitrary setting of the temperature change between liquid He and room temperature, quick exchange of the specimen and low consumption of liquid helium. We therefore chose

a combination of the double path interferometer (involving easy optical alignment³) and a continuous flow type cryostat (providing versatility in terms of temperature control and specimen set-up) for the present dilatometer system.

Figure 3 shows a schematic diagram of the present system. The cryostat system is composed of a continuous flow cryostat, a liquid helium reservoir with a flexible transfer tube, a gas flow controller with a diaphragm pump, and an oil diffusion vacuum pump. The interferometer system is set up on a vibration free base plate. The cryostat is suspended by a side arm, which is firmly fixed to a cylindrical column on the base plate. The cryostat is composed of a vacuum jacket, a He flow tube and a specimen cell. The vacuum jacket is made of Al with a vacuum-tight optical window beneath the bottom end, the inside of which is evacuated to high vacuum by an oil diffusion vacuum pump system. The cooling head, which is made of Cu and located at the bottom part of the helium flow stainless steel double tube, houses an electrical heater cemented by epoxy (Stycast 2850GT), and a silicon diode thermometer as a temperature control sensor. The specimen cell is located beneath the bottom of the cooling heat within double thermal guards, which are made of thin Al tubing. These guards are anchored at suitable positions on the flow tube.

A schematic diagram of the specimen cell is shown in Figure 4. The cell is designed to meet the requirements of good thermal uniformity and easy handling of the specimen. The vacuum cell is made of copper and its surface is gold plated to prevent any excess thermal radiation from the outside. The cell is fastened with an indium seal to the upper flange, which firmly comes into contact with the cold head. The cell is filled with a little helium exchange gas, for example at ≈ 100 Pa at room temperature, through a small inlet at the flange. A frame with a hole for the Rh-Fe thermometer is fastened to the same flange. The specimen and the two optical reflectors are made to optically contact one another and are lightly held on the frame by a small Be-Cu alloy spring. The rectangular reflectors are made of fused silica (dimensions 8×20 mm² and 2 mm thick; parallelism within 5 sec.; flatness within $\lambda/10$; Al thin coating film). The BK7 (borosilicate glass) optical window (dimensions 25 mm in diameter and 4 mm thick; parallelism within 5 sec.; flatness within $\lambda/10$) is fastened to the

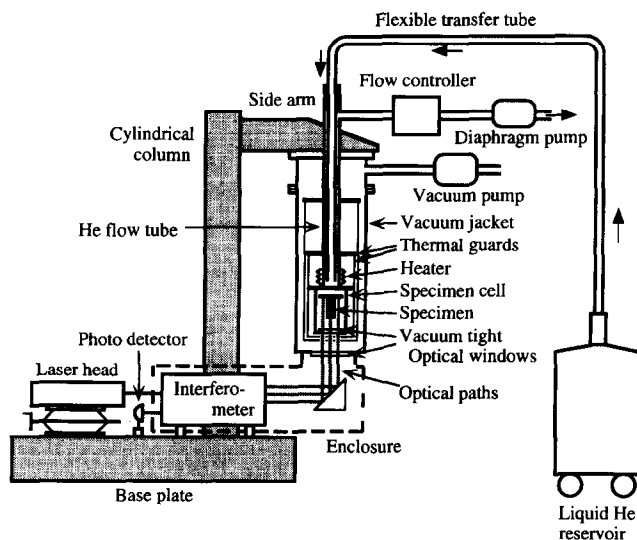


Figure 3 Mechanical arrangement of dilatometer

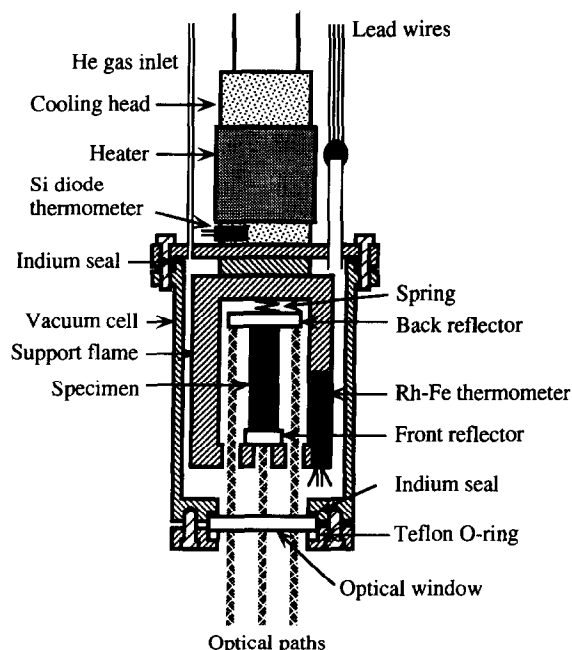


Figure 4 Details of specimen cell

bottom part of the cell with an indium seal and a Teflon O-ring.

A silicon diode thermometer (Lake Shore Cryotronics Inc., DT-470-SD-13) is used for controlling the temperature of the cold head in this system. A PID temperature controller (Lake Shore Cryotronics Inc., DRC-91CA), the set point resolution of which is 0.01 K, is coupled to the silicon diode thermometer to achieve various temperature changing modes, such as a continuous heating/cooling rate mode, or a step-like mode. The flow rate of helium vapour is controlled to be at constant values in certain temperature ranges using a thermal mass flow controller (Kojima Seisakusho Ltd, Model 3620, CR700) and a diaphragm pump (Sinku Kiko Ltd, DA-20D; speed of evacuation 20 dm³ min⁻¹). The flow rate is fixed to 3.0 dm³ min⁻¹ at 10–70 K, 0.8 dm³ min⁻¹ at 40–160 K and 0.4 dm³ min⁻¹ at 140–300 K in this experiment. The temperature of the cooling head is controlled by the heater, so that the specimen can be kept stable at any temperature in the range 5–300 K with a stability of ± 5 mK over many hours.

A Rh-Fe resistance thermometer (3.2 mm in diameter and 30 mm long, $\approx 30 \Omega$ at 300 K) used to determine the absolute temperature of the specimen was calibrated with an accuracy of better than 5 mK, including reproducibility, in the temperature range 5–300 K. The thermometer is inserted into a hole drilled in the Cu frame of the cell. Its output is measured by an automatic resistance bridge (Automatic System Laboratories Ltd, F26B). The operating frequency and current of the bridge are 75 Hz and 1.0 mA, respectively.

The levels of uncertainty for the measurement system are summarized in Table 1. Each uncertainty is calculated in terms of the contribution to the thermal expansion coefficient. As seen in Table 1, the dominant source of uncertainty is the fringe determination ambiguity.

Measurement results of fused silica SRM 739

The supplied material (originally in a cylindrical shape, 6.4 mm in diameter and 51 mm long) was cut into two dif-

Table 1 Sources and estimated values of uncertainty for 10 mm long specimens over a 10 K temperature interval

Source	Type	Amount	Contribution to expansion coefficient (K ⁻¹)
Laser frequency stability	Random	2 × 10 ⁻⁹	4 × 10 ⁻¹⁰
Fringe determination	Random	1 nm	1 × 10 ⁻⁹
Repeatability of zero drift of fringe fraction with temperature change	Random	0.05 nm K ⁻¹	5 × 10 ⁻⁹
Temperature determination	Random	10 mK	1 × 10 ⁻³ × α (max. value ^a = 1 × 10 ⁻⁹)
Temperature calibration	Systematic	5 mK	5 × 10 ⁻⁴ × α (max. value ^a = 5 × 10 ⁻¹⁰)
Determination of specimen length	Systematic	5 μm	2 × 10 ⁻⁴ × α (max. value ^a = 2 × 10 ⁻¹⁰)

^a The maximum value of the uncertainty is calculated using the maximum LTEC of the fused silica |α| = 1 × 10⁻⁶ K⁻¹

ferent length specimens, both ends of which are polished to be flat (flatness within λ/10) and mutually parallel (parallelism within 5 sec.) and give final lengths of 10 and 20 mm, respectively.

The dilatometer measurement was carried out as follows. At first, the specimen was cooled to the lowest temperature (usually below 10 K). The expansion ΔL_m (= L₂ - L₁) was measured between two temperature equilibrium states (T₁ and T₂). The typical temperature interval (ΔT) was selected to be 5 K below 60 K, 10 K at intermediate temperatures, and 15 K above 150 K.

This measurement cycle was repeated several times with each specimen. The measured length change ΔL_m has, in practice, three components: the specimen ΔL_{sp}, the front reflector ΔL_{FR} and an extra zero drift ΔL_{zd}, such that

$$\Delta L_m = \Delta L_{sp} + \Delta L_{FR} + \Delta L_{zd} \quad (2)$$

ΔL_{zd} might be due to optical misalignment caused by thermal deformation of the cryostat or deformation of the optical window by thermal stress. The effect of ΔL_{zd} can be cancelled by measuring the different length specimens, if ΔL_{zd} is reproducible between different experimental runs. If two specimens of 10 and 20 mm length are measured, each measured value (ΔL_{m1} and ΔL_{m2}) is determined as follows

$$\Delta L_{m1} = \Delta L_{sp(L=10\text{ mm})} + \Delta L_{FR} + \Delta L_{zd} \quad (3)$$

$$\Delta L_{m2} = \Delta L_{sp(L=20\text{ mm})} + \Delta L_{FR} + \Delta L_{zd} \quad (4)$$

As a result of subtracting Equation (3) from Equation (4)

$$\Delta L_{sp(L=20\text{ mm})} - \Delta L_{sp(L=10\text{ mm})} = \Delta L_{m2} - \Delta L_{m1} \quad (5)$$

is obtained, where the left-hand side means the 'net' length change of the 10 mm length specimen. Actually, we do not need to obtain values for the terms ΔL_{FR} and ΔL_{zd}. However, it is of interest to estimate the level of ΔL_{zd} from an experimental point of view. The maximum value of ΔL_{zd} in this experiment is estimated to be ≈1.4 nm K⁻¹ using a value of ΔL_{FR} given by another individual experimental run. This value makes a correction to the LTEC of ≈0.07 × 10⁻⁶ K⁻¹.

The corrected expansion data, obtained by the process

mentioned above, are plotted as open circles in Figure 5. The measured data from our middle temperature dilatometer are also shown, as solid circles^{5,6}. The present result is interpolated with the following empirical function

$$\alpha/10^{-6} \text{ K}^{-1} = a(b/T)^c \exp(b/T)/(\exp(b/T) + 1)^2 + d(e/T)^2 \exp(e/T)/(\exp(e/T) - 1)^2 \quad (6)$$

where: a = -4.22 ± 0.07, b = 35.5 ± 0.8, c = 0.335 ± 0.015, d = 1.253 ± 0.022 and e = 535 ± 9. These parameters were determined using a recursive least squares method. Equation (6) is useful, as only five parameters are sufficient to describe such an unusual temperature dependent curve. The first term of Equation (6), showing the negative expansion at lower temperatures, becomes a Schottky function if a > 0 and c is exactly equal to 2. And the second term, showing the positive expansion at higher temperatures, is an Einstein function. The Einstein's characterized temperature in this fit is calculated to be 535 K, which is comparable to the Debye temperature of 494 K given by Stephens⁸.

In general, another sort of correction in the fitting curve associated with a finite temperature interval measurement should be made^{9,5}. This is because, strictly speaking, an instantaneous thermal expansion coefficient, α = dL/(L₀dT), is not numerically equal to a 'measured' average thermal expansion coefficient $\bar{\alpha} = \Delta L/(L_0 \Delta T)$. However, such a cor-

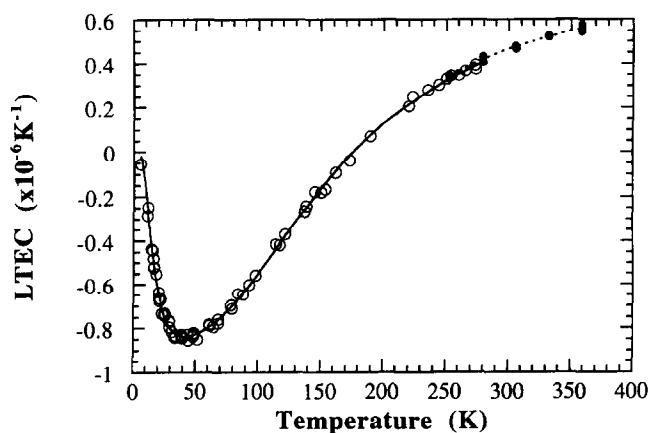


Figure 5 Measurement results of fused silica SRM 739: ○, present data; ●, references 5 and 6

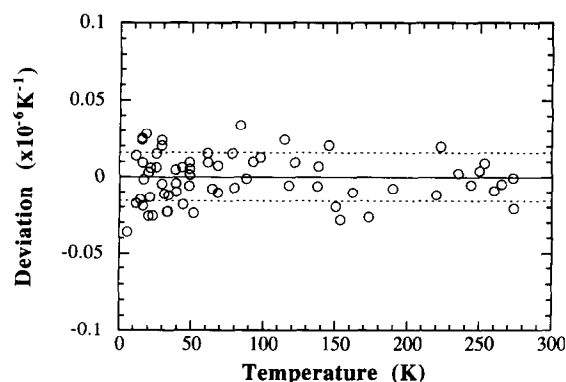


Figure 6 Deviation of data from fitting Equation (6) (dotted line represents the standard deviation of each data point)

Table 2 Generated smooth values of LTEC from the fit [Equation (6)]

T (K)	LTEC	T (K)	LTEC
6	-0.021	120	-0.391
10	-0.175	130	-0.312
15	-0.442	140	-0.236
20	-0.634	150	-0.165
25	-0.744	160	-0.097
30	-0.802	170	-0.035
35	-0.829	180	0.023
40	-0.838	190	0.077
45	-0.837	200	0.127
50	-0.829	210	0.172
55	-0.816	220	0.214
60	-0.799	230	0.253
70	-0.754	240	0.289
80	-0.695	250	0.322
90	-0.627	260	0.352
100	-0.551	270	0.381
110	-0.471	273	0.389

rection was not performed, because the maximum value of the correction is estimated to be $0.006 \times 10^{-6} \text{ K}^{-1}$ at the lowest temperature end and it decreases rapidly with temperature; and such values are smaller than the scatter of the data.

The deviation of each data point from the fitting function (6) is shown in Figure 6. The standard deviation of the data from the fit is calculated to be $0.016 \times 10^{-6} \text{ K}^{-1}$. The scatter of the data is mainly attributed to the imprecision of the length measurement, because that of the thermometry does not matter in the case of a low expansion material such as fused silica. The standard deviation is equivalent to a length measurement error of $\approx 2\text{--}3 \text{ nm}$. This value is comparable to the periodic error ($\pm 1 \text{ nm}$) for the interferometer output.

The present results, calculated from Equation (6) and listed in Table 2 are compared with some reported data. The deviations of previous data (Kirby and Hahn⁷, 80–273 K; Aikawa *et al.*¹⁰, 65–273 K; Drotning², 100–273 K; Okaji *et al.*^{5,6}, 253–273 K; White and Birch¹¹, 10–80 K) from the present fit are shown in Figure 7. The present results agree with the NIST certified values given by Kirby and Hahn⁷ over the range 80–273 K within $0.025 \times 10^{-6} \text{ K}^{-1}$, which is within the scatter levels of both measurements. The results by Aikawa *et al.*¹⁰ in the range 65–273 K agree with the present data within $0.025 \times 10^{-6} \text{ K}^{-1}$. The data measured by Drotning² are systematically lower than the present data, and the deviation finally reaches $0.05 \times 10^{-6} \text{ K}^{-1}$ at 100 K.

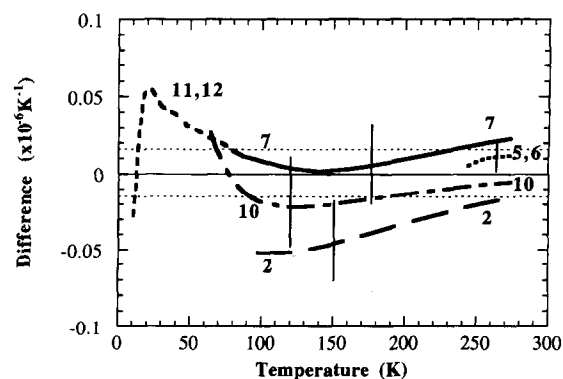


Figure 7 Comparison of present data and previously reported data (figures represent the reference numbers) from Kirby and Hahn⁷, 80–273 K; Aikawa *et al.*¹⁰, 65–273 K; Drotning², 100–273 K; Okaji *et al.*^{5,6}, 253–273 K; White and Birch^{11,12}, 10–80 K

Comparison of the present data with results for around room temperature (253–273 K) using our other dilatometer^{5,6} shows excellent agreement, within $0.01 \times 10^{-6} \text{ K}^{-1}$. The differences between the present data and the data of references 7, 10, and 5 and 6 are not statistically significant because the standard deviation of these data are reported to be $0.026 \times 10^{-6} \text{ K}^{-1}$, $0.03 \times 10^{-6} \text{ K}^{-1}$ and $0.009 \times 10^{-6} \text{ K}^{-1}$, respectively. No reported data have been found for this material below 65 K, so we compared the present results with data based on certain types of vitreous silica materials measured by White and Birch^{11,12}. The difference between the data sets reaches $0.05 \times 10^{-6} \text{ K}^{-1}$ around 20 K, but this discrepancy is natural, because these materials should have different characteristics to the reference fused silica.

Summary

We have developed a cryogenic dilatometer which covers the temperature range 5–300 K. A nanometer-order precision in length measurement has been achieved by means of optical heterodyne interferometry. The performance of the dilatometer was established by measuring fused silica SRM 739 specimens, and LTEC data are obtained in the range 6–273 K with a standard deviation of $0.016 \times 10^{-6} \text{ K}^{-1}$. The present result shows agreement with the literature values for SRM 739 within $0.05 \times 10^{-6} \text{ K}^{-1}$ in the range 65–273 K. Further work using an improved interferometer is in progress.

References

- 1 Roberts, R.B. *J Phys E: Sci Instrum* (1981) **14** 1386–1388
- 2 Drotning, W.D. *Int J Thermophys* (1988) **9**(5) 849–860
- 3 Okaji, M. and Imai, H. *J Phys E: Sci Instrum* (1984) **17** 669–673
- 4 Okaji, M. and Imai, H. *J Phys E: Sci Instrum* (1987) **20** 887–891
- 5 Okaji, M. and Birch, K.P. *Metrologia* (1991) **28** 27–32
- 6 Okaji, M. and Imai, H. *Netsu Bussei* (1992) **6** 83–88 (in Japanese)
- 7 Kirby, R.K. and Hahn, T.A. NBS Certificate SRM 739: Fused silica thermal expansion, National Bureau of Standards, Boulder, CO, USA (1971)
- 8 Stephens, R.B. *Phys Rev B* (1976) **13**(2) 852–865
- 9 Bennett, S.J. *J Phys E: Sci Instrum* (1977) **10** 525–530
- 10 Aikawa, H. Okaji, M. and Imai, H. *J Soc Instrum Cont Eng* (1991) **29**(12) 1131–1138 (in Japanese)
- 11 White, G.K. and Birch, J.M. *Phys Chem Glasses* (1965) **6**(2) 85–89
- 12 White, G.K. *Thermochimica Acta* (1993) **218** 83–99